Reprinted from Analytical Chemistry, 1985, 57, 1917.

pH-Based Enzyme Potentiometric Sensors. Part 1. Theory

Steve D. Caras[1] and Jiří Janata*

Department of Bioengineering, University of Utah, Salt Lake City, Utah 84112

Dietmar Saupe[2] and Klaus Schmitt

Department of Mathematics, University of Utah, Salt Lake City, Utah 84112

A diffusion-kinetic model for a pH based, one substrate, enzymatically coupled field effect transistor has been developed. The model includes one mobile buffer and has been solved for both transient and steady-state response. It is shown that the detection limit, slope, dynamic range, and time response are affected mainly by the buffer capacity and by the transport properties of all species involved.

Combination of a highly specific enzymatic reaction with a field effect transistor yields a new type of biosensor—ENFET. The purpose of this paper is to develop a general model which will predict the performance parameters of this device and will allow the optimization of its performance. The characteristic features of this model are similar to those describing a potentiometric enzyme electrode. The conclusions drawn from this model are, therefore, generally applicable to enzyme electrodes. In the following papers of this series this model, adjusted to the specifics of the glucose and benzylpenicillin enzyme reactions, is verified experimentally.

The literature concerning the enzymatic potentiometric sensors is extensive but limited mainly to enzyme electrodes. There are several excellent reviews of this subject (*1–3*). There have been only a few ENFETs reported in the literature (*4–7*).

THEORY

The schematic of the model of a potentiometric enzyme sensor (e.g., ENFET) is shown in Figure 1. There are two boundaries which are important: the zero flux boundary at the transistor surface ($x = 0$), and the solution/gel boundary ($x = L$) through which all species involved (except the enzyme) can freely pass.

The simplest model involves a pH-dependent enzyme reaction involving only one product pathway (Scheme I).

In this paper we assume that $\alpha = \beta = 1$ which implies that the Michaelis–Menten kinetics is pH-independent. There is a mobile buffer of a total concentration A_T, substrate S, product P, and proton H^+. The latter determines the pH at the transistor surface, which is experimentally observable.

The problem can be described by the general diffusion-reaction equation which for unidirectional geometry has a form

$$\frac{\partial c_1}{\partial t} = D_i \frac{\partial C_1}{\partial x^2} \pm R(C_i) \tag{1}$$

in which C_i is the concentration of species i, D_i is its diffusion coefficient, and R is the reaction term. For the substrate S eq 1 can be expanded to give

$$\frac{\partial [S]}{\partial t} = D_S \frac{\partial^2 [S]}{\partial x^2} - \frac{V_M [S]}{\left[1 + \frac{[H^+]}{K_{es_1}} + \frac{K_{es_2}}{[H^+]}\right](K_S + [S])} \tag{2}$$

Scheme I

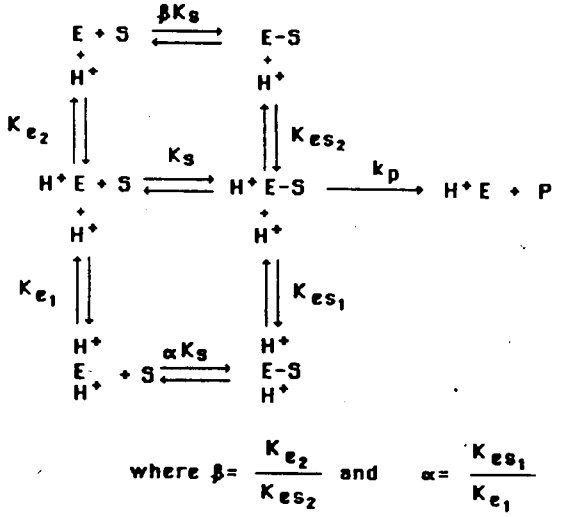

where V_M is the maximum reaction velocity and K_S The boundary and initial conditions are

$$S_x(0,t) = 0 \qquad S(L,t) = S_B \qquad S(x,0) = 0 \tag{3}$$

These equations can be normalized by letting

$$t = \bar{t}L^2/D_S \qquad [S] = C_S K_S \qquad x = \bar{x}L \tag{4}$$

where $\bar{t}$, C_S, C_p, and $\bar{x}$ are dimensionless variables. Substituting these relationships to eq 2 yields

$$\frac{\partial C_S}{\partial \bar{t}} = \frac{\partial^2 C_S}{\partial \bar{x}^2} - \phi^2 \frac{C_S}{1 + C_S} \tag{5}$$

where ϕ is the so-called Thiele modulus

$$\phi = L\left[\frac{V_M}{K_S D_S\left[1 + \frac{[H^+]}{K_{es_1}} + \frac{K_{es_2}}{[H^+]}\right]}\right]^{1/2} \tag{6}$$

Various models for enzyme electrodes have been solved over the years. The steady-state response of one substrate–one product, Michaelis–Menten kinetics have been obtained analytically (*8, 9*). Both transient and steady-state solution have been obtained by orthogonal collocation (*10*) and by the infinite series solution (*11*). The effect of the formation of the depletion layer at the solution/gel interface has been included in the model (*12–14*). The effect of mobile buffer has not been taken into account in either of these papers.

Our model (Figure 1) is based on the following assumptions:

(1) The gel matrix has no buffer capacity of its own and it is not charged. There is no Donnan effect.

(2) There is no depletion layer at the gel/solution boundary, the transport inside the gel is by diffusion only.

(3) Partitioning between the bulk of solution and the gel can occur for all species. Thus, the boundary concentrations

[1] Present address: Naval Research Laboratory, 4555 Overlook Ave., SW, Washington, DC 20375.
[2] Present address: FSP Dynamische Systeme, Universitat Bremen, D-2800 Bremen, West Germany.

0003-2700/85/0357-1917$01.50/0

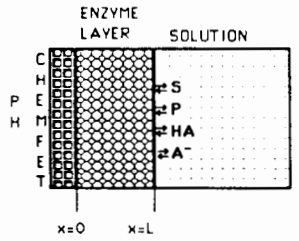

Figure 1. Diagram of the ENFET model.

at $x = L$ are the concentrations just inside the gel layer.

(4) There is no inhibition other than that by H^+.

(5) The total buffer concentration throughout the gel layer is constant.

(6) The protonation reactions are fast compared to all other processes.

(7) The diffusion coefficient of the substrate and of the product are equal. The diffusion coefficients of the protonated and unprotonated buffer are also equal.

(8) The response of the potentiometric sensor is fast.

Under these assumptions the following equation applies:

$$\frac{\partial[H]_T}{\partial t} = D_{H^+}\frac{\partial^2[H^+]}{\partial x^2} + \frac{V_M[S]}{\left[1 + \frac{[H^+]}{K_{es_1}} + \frac{K_{es_2}}{[H^+]}\right](K_S + [S])} + D_{HA}\frac{\partial^2[HA]}{\partial x^2} \quad (7)$$

where $[H]_T = [HA] + [H^+]$ and $[A]_T = [HA] + [A^-]$. The buffer equilibrium is described by its dissociation constant

$$K_{a_1} = \frac{[H^+][A^-]}{[HA]} \quad (8)$$

Equation 8 is solved for $[H^+]$ using the $[H]_T$ and the $[A]_T$ relationships; first and second space derivatives are calculated and inserted into eq 7.

The assumptions of the model determine the boundary

$$S_x(0,t) = H_x(0,t) = HA_x(0,t) = 0$$
$$S(L,t) = S_B \qquad HA(L,t) = HA_B \quad (9)$$
$$H(L,t) = H_B \qquad A(L,t) = A_B$$

and the initial conditions

$$HA(x,0) = HA_B \qquad S(x,0) = 0 \text{ for } x < L$$
$$A(x,0) = A_B \qquad H(x,0) = H_B \quad (10)$$

The resulting partial differential equations were solved by the method of lines in one dimension (MOL1D). It is a numerical technique suitable for solving parabolic and hyperbolic initial boundary value problems in one dimension. It uses a finite differences method to approximate the space derivatives and solves the resulting system of ordinary differential equations by using either Adams–Bashford–Moulton or Gear's method for stiff equations (*15*). Because the concentration profiles change most rapidly near the $x = L$ boundary, it was desirable to space the lines more closely at this boundary. However the MOL1D package does not support a variable mesh size. It was, therefore, necessary to transform the distance variable x into another variable using the relationship

$$y = L(1 - e^{-ax} + xe^{-a}) \quad (11)$$

This transformation allows for equal distribution in the y space while concentrating the lines close to the $x = L$ boundary. Parameter a sets the spacing of the lines. For our simulation it was set equal to five.

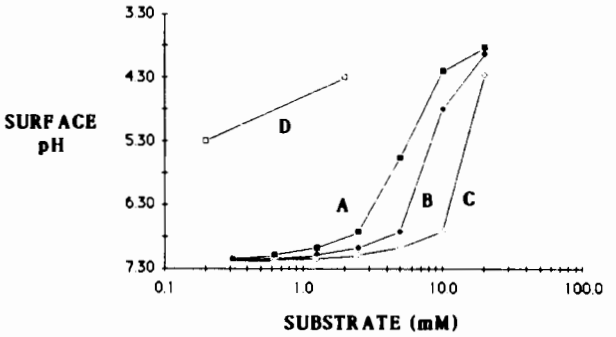

Figure 2. Theoretical calibration curves for three buffer concentrations: A 1 mM; B, 2 mM; C, 4 mM. D is the unit slope line. Diffusion coefficients ($\times 10^{-6}$ cm^2 s^{-1}) were $D_S = 1.0$, $D_{A^-} = 1.0$, and $D_H = 10$, $V_M = 3.2 \times 10^{-6}$ M cm^{-3} s^{-1}, length was 100 μm, and pH 7.20.

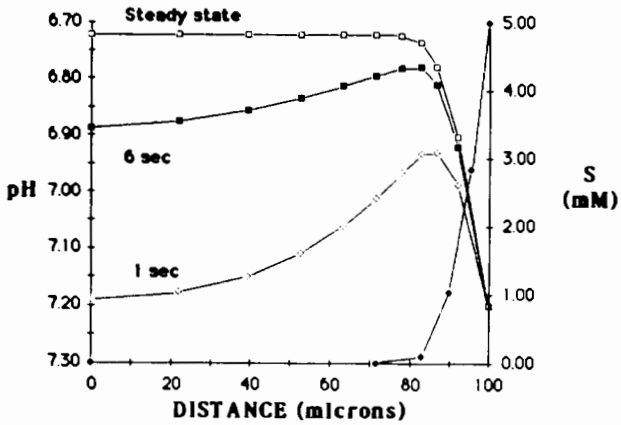

Figure 3. Time dependence of the concentration profiles for the substrates S (the initial concentration 5 mM) and of pH for the total buffer concentration 2 mM. Other parameters are identical with those given in Figure 2.

RESULTS

A rational classification of results can be obtained by examining a Thiele modulus (eq 6). In reality ϕ is a function of pH and of *all* diffusion coefficients. For $\phi > 10$ the mechanism is diffusion controlled. In order to assure the diffusion controlled regime, the value of ϕ was chosen to be 50.

Diffusion Limited Case. A series of calibration curves for three buffer concentrations are shown in Figure 2. It clearly indicates the profound effect that buffer capacity has on the slope, detection limit, and the dynamic range of the sensor. The concentration profiles through the gel layer for the substrate and for the hydrogen ion are shown in Figure 3. The surface pH (at $x = 0$) determines the response of the sensor. The effect of the substrate concentration on the concentration profile of the buffer anion (proton acceptor) is illustrated in Figure 4. It clearly shows that for high values of the substrate the buffer capacity of the gel is exceeded. The transient response of the ENFET is summarized in Figure 5.

Reaction Limited Case. In this case the value of ϕ is small. The diffusion fluxes of all species are then greater than the reaction term. Since ϕ is heavily dependent on the gel thickness, it has been adjusted to yield the reaction limited conditions by reducing the gel length by the factor of 10. The result is given in Figure 6 which shows that both the dynamic range and the slope are significantly reduced as compared with the equivalent experiment shown in Figure 2B.

DISCUSSION

The model presented in this paper corresponds to realistic conditions under which a potentiometric enzyme sensor would

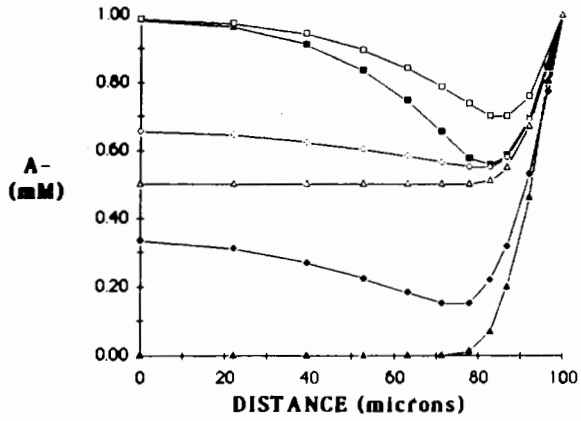

Figure 4. Time dependence of the concentration profiles for the buffer anion for two values of the substrate concentration: 5 mM (empty points), 10 mM (full points); (■) 1 s, (♦) 6 s, (▲) 40 s (steady state). The buffer concentration was 2 mM, other conditions were the same as those given in Figure 2.

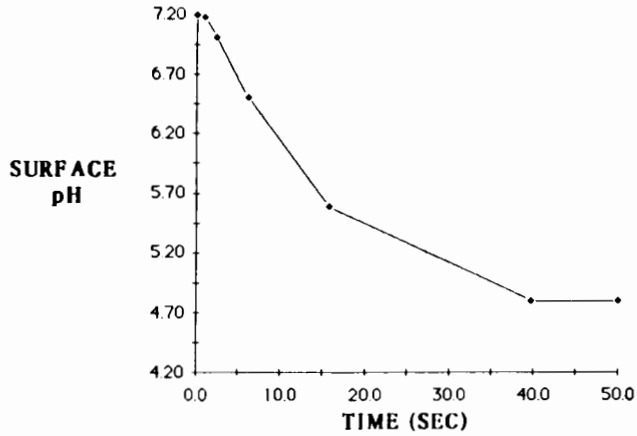

Figure 5. Theoretical time response of the ENFET for a step-change of the substrate concentration from 0 to 5 mM. Buffer concentration was 2 mM.

be expected to operate, namely, the presence of mobile buffer. If the buffer concentration is greater than 0.1 mM, the buffer capacity of the electrically neutral gel matrix with the immobilized enzyme can be neglected. We have chosen not to include a depletion layer at the gel/solution interface that corresponds to the experimental conditions of a well-stirred solution. We recognize that such conditions may not exist in, for example, in vivo measurements where the external mass transport would be limited.

The choice of the method-of-lines numerical integrator and the additional space transformation has been dictated by the order and stiffness of the partial differential equations. This method, which has been successfully used for solving a more complicated diffusion-kinetic model of the glucose ENFET (Part 2) and benzylpenicillin ENFET (Part 3), proved to be economical with respect to the required computing time. In principle, the depletion layer boundary could be incorporated into this model.

Results in Figure 6 clearly show that the only practical regime for operating a potentiometric enzyme sensor is under the diffusion control as has been noted by others (*1*, *3*, *10*, *11*, *13*). It also shows that enzymatic sensors with the enzyme immobilized only at the surface (*7*) ($x \sim 0$) are not practical. In the ensuing discussion we will, therefore, examine the response characteristics of the diffusion controlled case only.

The response of a potentiometric enzyme sensor is composed of two parts: the kinetic one which has its origin in the enzymatic generation of the ionic product (or consumption of ionic reagent) and the thermodynamic one which originates

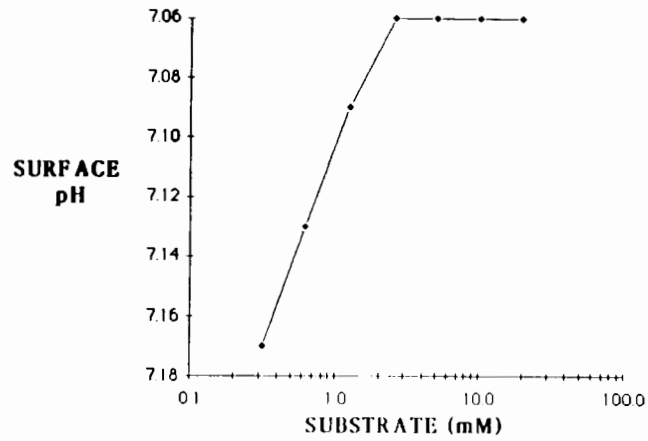

Figure 6. Theoretical calibration curve of the ENFET with 10 μm thick gel layer. Buffer concentration was 2 mM and other parameters were identical with those given in Figure 2.

from the Nernst potential which develops at the interface of the ion-selective sensor and the enzyme-containing layer. The experimental conditions (ionic strength and the gel matrix) are usually chosen such that the Donnan potential at the gel/solution interface is insignificant. Because of the presence of the nonthermodynamic component of the response, the Nernst slope has no special meaning with enzymatic sensors. This can be seen from Figure 2 in which the theoretical slope is as high as 6 decades of surface pH/1 decade of the substrate. Why this is so can be seen in Figure 4. The two sets of concentration profiles of the buffer anion correspond to the low and high end of the maximum slope region in Figure 2B. For the low substrate concentration there is an appreciable amount of A^- left at the transistor surface. However, as the substrate concentration increases the increased production of H^+ lowers the buffer capacity thus making the gel more susceptible to larger pH decrease. This will go on until the buffer capacity reaches its minimum value. Any further increase in substrate concentration will then produce a unit slope until the reaction velocity is reduced due to the pH-dependent Michaelis–Menten mechanism and the process becomes reaction controlled.

The detection limit cannot be predicted in general for all enzymatic sensors although our model allows us to calculate it for specific pH–based sensors (cf. parts 2 and 3). It is significantly affected by the buffer concentration (Figure 2). For the normal range of diffusion coefficients and for substrates of a medium molecular weight, the detection limit is approximately 0.1 mmol/L (*1–3*).

The time response is determined by the diffusion of all species within the gel layer (Figure 5). Approximately, the overall time constant consists of the time constant $\tau_s = L_s^2/D_s$, associated with the diffusion of the substrate and the time constant $\tau_b = L_b^2/D_b$, associated with the diffusion of the buffer. Subscripts s and b denote the effective reaction length and the effective buffer movement, respectively (Figure 3). If we take L_b as ~ 20 μm and L_s as 80 μm, the approximate time constant is 10.4 s as compared to 14 s from Figure 5.

The dynamic range in our model is limited only by V_M through the enzyme loading and by the enzyme pH activity curve. The effect of those parameters is the same as discussed by other authors (*10*).

LITERATURE CITED

(1) Guilbault, G. G. *Appl. Biochem. Biotechnol.* **1982** *7*, 85–98.
(2) Guilbault, G. G. *Enzyme Microb. Technol.* **1980**, *2*, 258–264.
(3) Kobos, R. "Ion Selective Electrodes in Analytical Chemistry"; Freiser, H., Ed.; Plenum Press: New York, 1980; Vol. 2, pp 1–84.
(4) Danielsson, B.; Lundstrom, I.; Mosbach, K.; Stilbert, L. *Anal. Lett. B* **1979**, *12*, 1189–1199.
(5) Caras, S.; Janata, J. *Anal. Chem.* **1980**, *52*, 1935–1937.
(6) Hanazato, Y; Shono, S. *Proc. Chem. Sensors* **1983**, 513–518.

(7) Miyhara, Y.; Matsu, F.; Moriizumi, T. *Proc. Chem. Sensors* **1983**, 501–506.
(8) Thomas, D.; Broun, G. *Biochemie* **1972**, **54**, 229–244.
(9) Blaedel, W. J.; Kissel, T. R.; Boguslaski, R. C. *Anal. Chem.* **1972** *42*, 2030–2037.
(10) Brady, J.; Carr, P. *Anal. Chem.* **1980**, *52*, 977–980.
(11) Hameka, H.; Rechnitz, G. A. *J. Phys. Chem.* **1983**, *87*, 1235–1241.
(12) Jochum, P.; Kowalski, B. *Anal. Chim. Acta* **1982**, *144*, 25–38.
(13) Gough, D.; Leypoldt, L. "Appl. Biochemistry and Bioengineering"; Academic Press: New York, 1981; pp 175–207.
(14) Morf, W. E. *Mikrochim. Acta* **1980**, *2*, 317–332.
(15) Hyman, J., Los Alamos National Laboratory, Computer Library.

RECEIVED for review January 22, 1985. Accepted April 5, 1985. The support of this project from the NIGMS, Grant No. GM 22952-08, is greatly appreciated.